Novelty Journals

ISSN 2394-9716

International Journal of Novel Research in Interdisciplinary Studies
Vol. 12, Issue 4, pp: (8-29), Month: July – August 2025, Available at: www.noveltyjournals.com

Optimization and Modelling of Adsorption of Heavy Metals from Wastewater using *Telfairia occidentalis* and brewer's spent grain eco-friendly adsorbents

Harriet Ifeoma Anyaene [1], Dominic Okechukwu Onukwuli [2], Nkiruka Justina Edeani[3]

[1]Caritas University, Amorji Nike Enugu State, Nigeria.

[2]Nnamdi Azikiwe University, Awka, Anambra State, Nigeria

[3]University of Agriculture and Environmental Sciences, Umuagwo, Imo State, Nigeria

DOI: https://doi.org/10.5281/zenodo.16370573

Published Date: 23-July-2025

Abstract: **In this work, the adsorption of heavy metal ions on Brewers' spent grain adsorbent (BSGA) and *Telfairia occidentalis* seed adsorbent (TOSA) was optimized and modelled kinetically. In a batch system, aqueous solutions were used to study the adsorption isotherms and kinetics of lead (Pb) and arsenic (As) ions onto TOSA and BSGA with reference to pH, adsorbent concentration, and settling time. The Design Expert version 12 was utilized in the response surface methodology (RSM) design of the experiment. According to experimental findings, the adsorption process was favoured by an acidic pH, increasing initial TOSA and BSGA concentrations, and longer settling times. For BSGA, the ideal dosage, pH, and settling time were found to be 4.12 g/l, 2.60, and 40.35 Min; for TOSA, they were 4.00 g/l, 4.00, and 40-min, respectively. The best removal efficiencies with BSGA were 63.33 per cent As and 83.37% Pb, and with TOSA, 86.36 per cent As and 85.37% Pb. The pseudo-first-order, pseudo-second-order, Elovich kinetic, and intra-particle diffusion model equations were applied to fit the experimental datasets for the adsorption of lead and arsenic ions under various conditions. From the model results, the rate constants of the first-order adsorption model (k_1), the second-order kinetic model (k_2), and the intra-particle diffusion rate constants ($k_{int.}$) were determined. The experimental data fitted both the pseudo-second-order kinetic models and the Langmuir isotherm model very well, indicating that chemisorption is the adsorption mechanism. It also followed the intra-particle diffusion model for 20 minutes, after which it deviated indicating that intra-particle diffusion was not the sole rate-controlling step.**

Keywords: **Adsorption, heavy metals, pollution, optimization, wastewater.**

1. INTRODUCTION

Heavy metal-related environmental contamination has grown to be a major issue on a global scale (Sall *et. al.,* 2020). When there are large concentrations of metallic elements in the environment which are harmful to people, animals, and plants, it is referred to as heavy metal pollution (Vandana & Poonam, 2023). According to Gupta *et. al.* (2023) and Ullah *et. al.* (2023), Pb, Hg, Cd, As, and Cr are the most frequently occurring heavy metals that cause contamination. According to Vo *et. al.* (2020), mining, industrial additives, pesticide and fertilizer use, inappropriate disposal of electronic waste, and vehicle

emissions are some of the causes of heavy metal contamination. Fish and other aquatic species may perish as a result of heavy metal contamination of aquatic environments (Alalwan *et. al.,* 2020). According to Singh *et. al.,* (2024), those who come into touch with contaminated water may experience skin irritation as well as other health issues. Children who are exposed to heavy metals in food crops may experience major health issues such as cancer, neurological diseases, and developmental delays. Because heavy metals are non-biodegradable, they accumulate in the environment in contrast to organic molecules (Bayero *et. al.,* 2020; Sall *et. al.,* 2020). One of the things that contribute to heavy metal pollution of water resources is the paint industry activities. Paint industry is one of the biggest consumers of water in manufacturing processes (Ayawei *et. al.,* 2017). Wastewater generated during the paint-making process is a big environmental problem (Mathur & Sherry, 2023). The paint business produces wastewater that contains a variety of organic and chemical substances that are unhealthy for the environment and other living things (Rana *et. al.,* 2022). According to Ainul & Nazirah, (2020); Vishali & Kavitha, (2021), the primary causes of wastewater from the paint industry are cleaning operations, equipment maintenance, product changes, and spoilage. According to Aboulhassan *et. al*. (2014) and Chukwuma *et. al.,* (2022) organic solvents, heavy metals, suspended particles, and colourful pigments are the primary contaminants found in paint effluent. The discharge of wastewater from paint companies that have not been effectively treated or has not been treated at all can seriously impact human health and aquatic life (Fahim & Said, 2023). Furthermore, the aesthetic value and visual appeal of water bodies may be adversely affected by the hue and opacity of the wastewater released.

Paint effluent contains heavy metals that can be harmful to the environment and human health, including arsenic, cadmium, lead, mercury, chromium, and cadmium (Joshi & Gururani, 2022; Kulkarni, 2016). According to Dagne (2020), lead (Pb) is among the metals that have the most detrimental effects on human health. Because Pb disturbs the delicate antioxidant balance in mammalian cells, it causes oxidative stress and plays a role in the pathophysiology of Pb contamination. Anaemia, headaches, stomach aches, brain damage, and disorders of the central nervous system are all brought on by high levels of lead buildup in the body (Rehman *et. al.,* 2013; Saini *et. al.*, 2020; Abugu *et. al.,* 2023). The chemical element arsenic (As) has an atomic number of 33. One substance that poses a risk to human health and the environment is arsenic (Shrestha *et. al.,* 2021). Contaminated groundwater poses the biggest risk to public health when it is contaminated with As (Najamuddin *et. al.,* 2021). Exposure can come from contaminated drinking water, irrigated crops, and food cooked with contaminated water (Podgorski & Berg, 2020). Abdominal pain, a strong headache, vomiting, thickening of the skin on the palms and soles of the hands, irregular heart beat, and skin discolouration are a few signs of arsenic poisoning (Batool *et. al.*, 2024).

Heavy metals can be economically and environmentally removed from wastewater by adsorption utilizing, biosorbents (Chakraborty *et. al.,* 2022). Biosorbents are naturally occurring materials that may efficiently remove heavy metals from wastewater. Examples of these compounds include fungi, bacteria, and plant components. Therefore, to preserve the environment and adhere to legal requirements, wastewater from the paint industry must be effectively treated. Wastewater from the paint industry is often treated using physical, chemical, and biological treatment systems that take into account factors like pH, temperature, and pollutant concentration. An important area of research that can aid in the development of a sustainable heavy metal removal approach is the optimization of the adsorption of heavy metals from paint wastewater using biosorbents (Mwaniki *et. al.*, 2019).

Telfairia occidentalis seeds (TOS), also referred to as fluted pumpkin seeds (Figure 1a), are potent natural biosorbents that effectively remove contaminants from contaminated water (Anyaene *et. al.* 2022). Because these seeds are inexpensive, readily available, and environmentally benign, biosorbents made from them have demonstrated the potential to be used in wastewater applications (Bilal et. al., 2021). Lignin, cellulose, hemicellulose, and pectin are among the active substances found in the seeds that help them function as biosorbents (Nyong *et. al*., 2021; Wirnkor *et. al.,* 2020). These substances can bind and attract a variety of contaminants as a result of their hydrophilic and hydrophobic characteristics. While the lignin content can interact with hydrophobic organic contaminants from contaminated water, the hydroxyl groups in cellulose and hemicellulose can interact with heavy metal ions through ion exchange mechanisms (Etale *et. al.,* 2023). Dyes like methylene blue and rhodamine B can be removed by seeds up to 95% of the time (Obiora-Okafo & Onukwuli, 2017). There are several advantages of using fluted pumpkin seeds as biosorbents instead of more traditional treatment techniques. These substances can bind and attract a variety of contaminants due to their hydrophilic and hydrophobic characteristics.

Novelty Journals

ISSN 2394-9716

International Journal of Novel Research in Interdisciplinary Studies
Vol. 12, Issue 4, pp: (8-29), Month: July – August 2025, Available at: www.noveltyjournals.com

Figure 1: (a) *Telfairia occidentalis* seeds **(b) Brewers spent grain.**

A byproduct of the beer brewing process is the brewer's spent grain, or BSG (Figure 1b) (Samuel *et. al.,* 2019; Schmidt *et. al.*, 2023). BSG is the solid leftovers from boiling, straining, and separating malted barley and other grains from the liquid wort required to make beer (Sana *et. al.,* 2019). In breweries, this amounts to a substantial waste stream. For every 100 litres of brewed bear, about 20 kg of wet BSG are produced (Lnch *et. al.,* 2016). Because it is a rich source of proteins, fibres, and minerals, it has the potential to be an invaluable resource for animal feed. Due to the large volume produced each year and the poor market value at the moment, further applications for BSG must be looked into. This is advantageous not only for the brewer, who stands to gain but also for the environment since it is becoming more and more crucial to recycle and reuse industrial wastes and by-products derived from agriculture. According to Sana *et. al.* (2017) and Lynch *et. al.*, (2016), it has a high dry basis content of cellulose (12–25%), hemicellulose (20–25%), lignin (12–28%), and protein (19–30%), all of which increase its potential as an adsorbent in wastewater purification. While Yi *et. al.,* (2021) researched recycling BSG as an adsorbent by nitro-oxidation for uranyl ion removal from wastewater, Samuel *et. al.,* (2019) investigated the utilization of BSG in the treatment of electroplating effluents.

It is crucial to model the adsorption process, particularly in water treatment operations. Mathematical models are utilized to ensure that the suitable adsorbent is used to remove the target pollutant in water with good efficacy at the right rate and under precise conditions. These models also provide invaluable information that can be used to build an adsorption reactor for large-scale adsorption applications.

The link between a substance's concentration in the liquid phase and its amount adsorbed onto the solid phase at equilibrium is displayed via adsorption isotherms (Ahmad *et. al.*, 2015; Ayawei *et. al.*, 2017). Adsorption is used in paint wastewater treatment to extract contaminants from water by employing biosorbents.

Promising outcomes have been observed in the treatment of paint wastewater by the use of biosorbents, which are efficient in eliminating several contaminants usually present in paint wastewater, including organic compounds and heavy metals. Three widely used isotherm models to describe the adsorption of molecules onto a surface are the Langmuir, Freundlich, and Temkin isotherms. The Langmuir isotherm model postulates that only one molecule can adsorb at a time (monolayer adsorption) at each adsorption site, and that adsorption takes place on a homogenous surface with a finite number of identical adsorption sites with a high adsorption energy (Maftouh *et. al.*, 2023). The linear equation for the Langmuir model is shown as Equation 1.

$$\frac{C_e}{q_e} = \frac{1}{q_{max} K_L} + \frac{1}{q_{max}} C_e \quad (1)$$

Where, qmax is the maximum amount of the molecule that can be adsorbed per unit mass of the adsorbent; Ce is the concentration of the molecule in solution; and K_L is the Langmuir constant, which is associated with the adsorption sites' affinity for the molecule.

According to the Freundlich model, adsorption takes place on heterogeneous surfaces with different numbers of adsorption sites. Furthermore, according to Adegoke *et.al.*, (2023), adsorption onto one surface is presumed to be independent of adsorption onto other sites. Equation 2 provides the equation's linear form.

$$lnqe = \frac{1}{n} ln\, Ce + ln\, K_F \quad (2)$$

where qe is the number of molecules adsorbed at equilibrium per unit mass of adsorbent, and Ce is the equilibrium concentration of molecules in solution. The adsorbent's adsorption capacity is determined by the Freundlich constant (K_F), whereas the heterogeneity of the adsorption sites is determined by the Freundlich exponent (n).

The treatment of paint effluent using biosorbents provides an economical and environmentally friendly way to remove pollutants. Gaining insight into the adsorption isotherms involved in this procedure can enhance and optimize the treatment process.

According to the Temkin isotherm model, adsorption takes place on a surface where the adsorption energy is distributed uniformly. Equation 3 represents the Temkin model.

$$qe = (\frac{RT}{B_T}) ln\,(ACe) \quad (3)$$

where Ce is the concentration of molecules in solution at equilibrium, qe is the number of molecules adsorbed per unit mass of the adsorbent at equilibrium, and A and B are the Temkin constants, which are associated with the heat of adsorption and the strength of adsorption, respectively.

The mass transfer mechanisms, adsorbent performance, and adsorption rate are all covered in the adsorption kinetics study. The design of adsorption systems requires knowledge of the adsorption kinetics.

Adsorption kinetics is used to quantify the diffusion of adsorbate in the adsorbent's pores. It is defined as the adsorption uptake concerning time at a constant pressure or concentration.

The major aim of this research was to remove heavy metals from paint industrial wastewater, applying eco friendly; locally sourced adsorbents. The objective of the current work was to remove lead and arsenic ions from paint effluent using an adsorption technique.

2. MATERIALS AND METHODS

2.1 Collection and preparation of samples

The paint plant at the Emene Industrial Layout Enugu, Enugu State, Nigeria, provided the paint wastewater (PWW) used in this analysis. Samples were brought to the lab in previously cleaned plastic containers. We bought mature pods with seeds of *Telfairia occidentalis* at the Abakpa market in Enugu Town, Nigeria. After being taken out of the pod, the seeds were dried for five days in direct sunshine before the outer shells w,ere peeled off. We used seeds that showed no evidence of excessive desiccation, discolouration, or softening. Using a standard food processor, the seed kernels were ground into a fine powder, which was then sorted using a 300 µm sieve. In the experiment, seed powder (TOSP) was utilized.

The source of the brewer's spent grains was Ama Brewery located at Ninth Mile Corner, Enugu. For five days, the powder was allowed to dry in the sun. A 300 µm sieve was used for classifying the dried powder. The experiments made use of the powder (BSGP). By mixing distilled water with the fine powder to create a 2% suspension (2 g of fine powder samples in 100 ml water), the active ingredients from each powder, TOSP, and BSGP, were extracted. To help with extraction, the suspension was constantly agitated for 30 minutes at room temperature with a magnetic stirrer. After that, it was filtered through sturdy filter paper. The filtrate solutions that were produced were employed as TOSA/BSGA adsorbents.

2.2 Characterization of TOSA and BSGA

Fourier transform infrared (FTIR) spectrophotometer (IR Affinity-1, Shimadzu Kyoto, Japan) was used to examine the adsorbent extracts. The 4000-400 cm-1 range was used to measure the spectra. The chemical structures and functional groups of the materials were investigated using infrared spectroscopy. The adsorbent extracts were subjected to surface structure analysis using a Phenom Prox., Phenom-World Eindhoven, Netherlands, scanning electron microscopy (SEM). Using energy-dispersive X-ray (EDX) spectroscopy, the elemental makeup of the samples was examined.

2.3 Characterization of paint wastewater

Standard solutions for lead, arsenic, and other metals under research were generated at three different concentrations (2.0, 4.0, and 6.0 ppm) to obtain a calibration curve by diluting a stock standard solution with a concentration of 1000 ppm. Wet digestion was applied to wastewater sample digestion. A 100 ml volumetric flask was filled with 30 ml of the samples, and 30 cm^3 of HNO_3 (Aqua regia) was then added. The mixture was left to stand for a few hours. After that, it was gradually heated in a water bath until the flask's red vapours stopped. After that, the flask was left to cool to room temperature. After adding 4.0 ml of perchloric acid and heating the flask over a water bath once more to evaporate a tiny amount, the volume was adjusted with deionized water until a 50 ml mark was attained. The mixture was then filtered through Whatman filter paper No. 42. To identify the heavy metals in the paint effluent, an Atomic Absorption Spectrometer model AA-7000 Shimadzu, Japan ROM version 1.01 with S/N A30664700709 was utilized. Hollow cathode lamps for As, Pb, Ni, Hg, Fe, Cu, and Cr (Shimadzu) were used as the radiation sources, and air acetylene was used as the fuel. All samples and standards were run in duplicate.

2.4 Batch Adsorption Process

Response surface methodology (RSM) was used in the design of experiments to investigate the impact of process factors on the adsorption process. The TOSPA/BSGA dosage (1–5) g, pH (2–8), and settling time (10–50) Min were the range of the process parameters. Paint effluent (100 ml) was added to a conical flask along with the necessary quantity of TOSPA/BSGA. A magnetic shaker was used to continuously agitate the contents of the flask at 150 rpm. The temperature used for the experiments was steady at 303 K. Using a graduated syringe, a 2 ml sample was taken after each experimental run to determine the equilibrium concentration. For every experiment, the starting and equilibrium lead concentrations were determined at a wavelength of 525 nm using a UV-visible spectrophotometer (Shimadzu Inc., Japan). After each experiment, the removal efficiency and the quantity of adsorbed Pb and As were determined using Eqs. (4) and (5), respectively.

$$Contaminant\ removal\ (\%) = \left(\frac{C_0 - C_e}{C_0}\right) X\ 100 \quad (4)$$

$$qt\ (mg/g) = \frac{(C_o - C_t)\ V}{M} \quad (5)$$

C_0 is the initial contaminant concentration (mg/l), C_t is the contaminant concentration at time t in the bulk solution (mg/l), V is the volume of the solution (l), and M is the coagulant mass (g/l).

2.5 Experimental design

A face-centred experimental plan was used as the central composite design (CCD) in this investigation. By selecting $\alpha = 1$, a CCD becomes face-centred (Montgomery, 2011). The star points at the cube portion of the design's face are located near the face centre (Myers & Montgomery, 1995). Given that face-centred CCD is an option in CCD design and that the design is laborious, it was chosen (Gadokar, 2019). Face-centering the CCD guarantees that the axial runs will not be more extreme than the factorial component. The study's independent variables included TOSA/BSGA concentration (A), pH (B), and settling time (C); the study's response variables were lead ion removal efficiency and arsenic ion removal efficiency. For each sample, a 2^3-level two-level factorial CCD was performed for three independent variables. This involved eight factorial points coded according to the standard ± notation, six axial points, and six replicates at the centre point. For every response, twenty trial runs were carried out. The total number of runs was calculated mathematically using Equation (6). With k factors, the total number of experiments, N, is

$$N = 2^k + 2.k + n \quad (6)$$

Where k is the number of factors and n is the centre point. The CCD-designed results were modelled using RSM. The independent factors and their coded values are listed in Table 1. The range of these values was obtained from preliminary one-factor-at-a-time (OFAT) experiments. The experimental data were fitted to a polynomial model equation (Equation 7).

$$Y = \beta_0 + \sum_{i=1}^{K} \beta_i X_i + \sum_{i}^{K} \beta_{ii} X_i^2 + \sum_{1}^{K} \sum_{i \neq j=1}^{K} \beta_{ij} X_i X_j + \varepsilon \quad (7)$$

Where Y is the predicted response, X_i and X_j are the input variables, and β_o, β_{ii}, and β_{ij} are the regression constants for the linear, quadratic, and interaction coefficients, respectively.

Table 1: Experimental factors and design

Variable	Factors	Level		
		-1	0	+1
BSGA/TOSA concentration	A	1	3	5
pH	B	2	4	8
Settling Time	C	10	30	50

3. RESULTS AND DISCUSSION

3.1 AAS analysis of the paint wastewater used in the analysis

Table 2 displays a metallic analysis of the raw paint effluent used in this investigation. The outcomes were contrasted with the Environmental Protection Agency (EPA) and World Health Organization (WHO) guidelines for the disposal of wastewater in the environment (land or aquatic bodies). The levels of lead and arsenic (2.2581 and 1.2500 mg/l, respectively) were found to be higher than the upper limit permitted by the EPA and WHO. This suggests that paint wastewater must be cleaned before being released into the environment to ensure public safety and environmental preservation.

Table 2: Physicochemical characteristics of Paint wastewaters

Parameters	PWW Before adsorption	WHO STD	EPA limit
Arsenic, mg/l	2.2581	-	0.5
Zinc, mg/l	0.0433	3.00	5.00
Lead, mg/l	1.2500	0.010	0.100
Nickel, mg/l	0.7179	-	1.00
Mercury, mg/l	0.000	0.002	0.01
Iron, mg/l	1.9563	0.300	10.00
Copper, mg/l	0.0000	2.00	1.00
Chromium, mg/l	0.1167	0.200	1.00

3.2 FTIR spectrum analysis of BSGA and TOSA

The FTIR spectra of TOSA and BSGA are displayed in Figures 2ai and 2aii. O-H and N-H stretching were identified as the cause of the large peaks at wave numbers 3693.8 cm-1, 3652.8 cm-1, and 3623.0 cm-1 (Silverstein & Bassler, 1962). The alcohol's O-H bending produced the band at 1420.1 cm-1. Because of the organic and inorganic components found in the brewer's leftover grain used in the study, there were about 17 discernible peaks. The C-H stretching of alkynes, C-H bending of aromatic compounds, O-H bending of alcohols, C-O stretching of esters, C-N stretching of amines, and C=C bending of alkenes were identified as the sources of the absorption peaks at 3276.3, 1836.3, 1420.1, 1319.5, 1237.5, and 913.2 cm-1, respectively. The involvement of functional groups during the adsorption process can be explained by the emergence and removal of these groups during the process. Figures 2bi and 2bii display TOSA's FTIR spectra before and following adsorption, respectively. Nineteen visible bands were used to characterize the spectrum. Aamide, N-H, and O-H stretching are represented by the bands at 3429.2 cm-1; O-H stretching and bending are represented by the bands at 3242.8 cm-1 and 1558.0 cm-1, respectively. N-H and O-H stretching was also the cause of the band at 2855.1 cm-1. O-H bending caused the bands at 1558.0 cm-1 and 1360.5 cm-1. The outcome demonstrated the organic and inorganic components of TOSA. Additional functional groups found in TOSA included C-H deformation, C-H bend, and C=O stretching.

Novelty Journals

ISSN 2394-9716

International Journal of Novel Research in Interdisciplinary Studies
Vol. 12, Issue 4, pp: (8-29), Month: July – August 2025, Available at: www.noveltyjournals.com

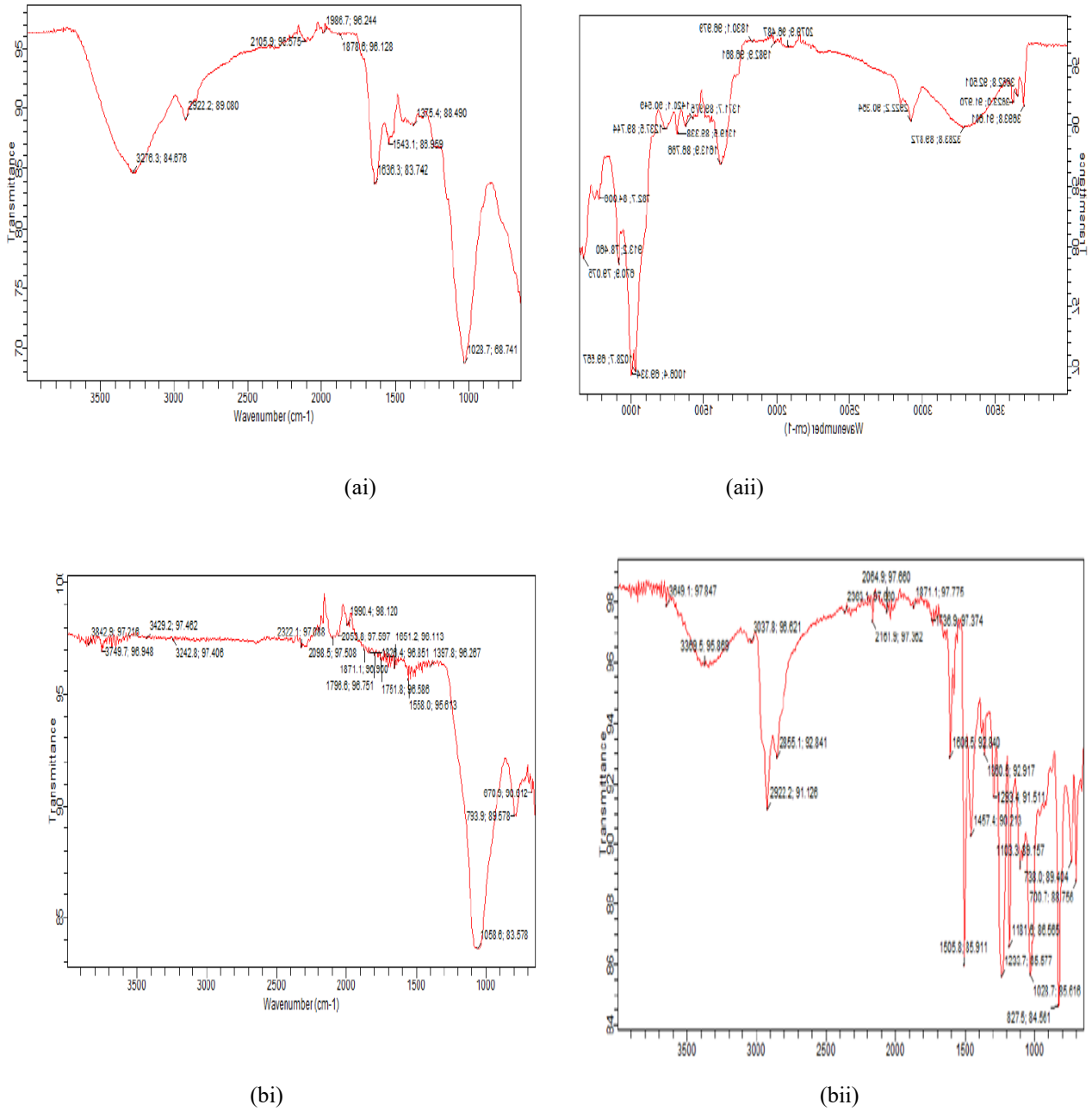

Figure 2: FTIR spectrum of BSGA and TOSPA: (ai and aii) BSGA before and after adsorption (bi and bii) TOSA before and after adsorption processes, respectively.

3.3 SEM image analysis of BSGA and TOSA

Plates 1 and 2 displayed the findings of the SEM pictures of TOSA and BSGA, respectively. The outcomes showed that the surfaces of TOSA and BSGA are rough-porous. The particles had a compact disk form that was uneven. The existence of pores in both BSGA and TOSA—mesopore, macropore, and micropore—proved their suitability as adsorbents. The adsorption process is aided by these pore spaces.

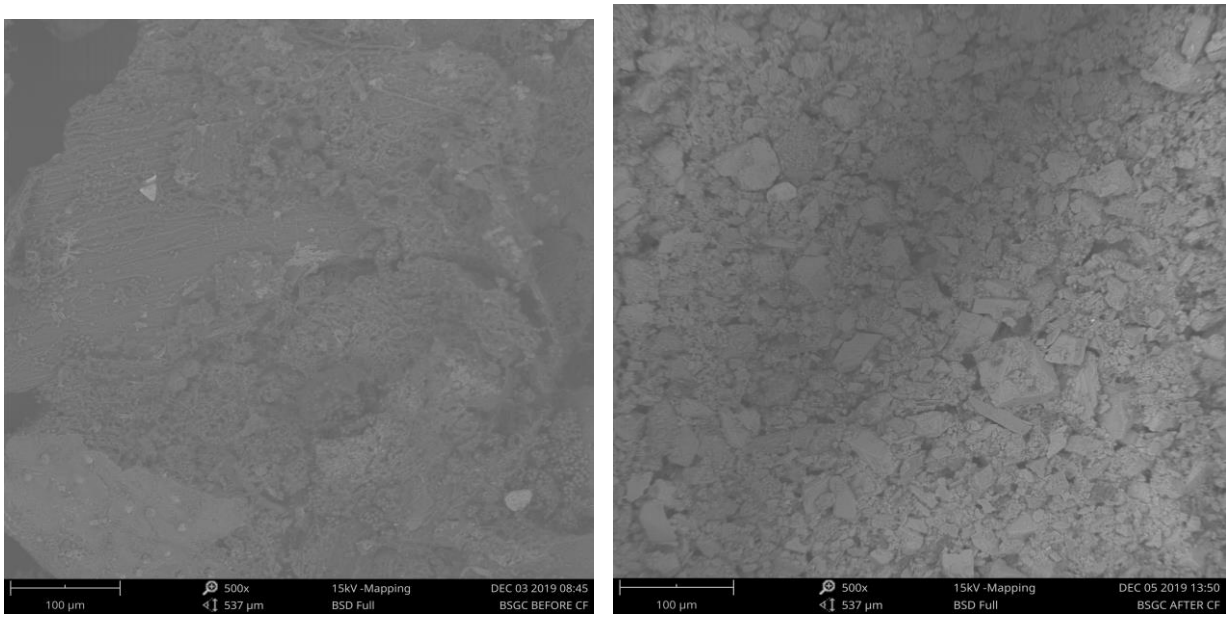

(a) **(b)**

Plate 1: SEM micrograph of BSGA (a) before adsorption (b) after adsorption.

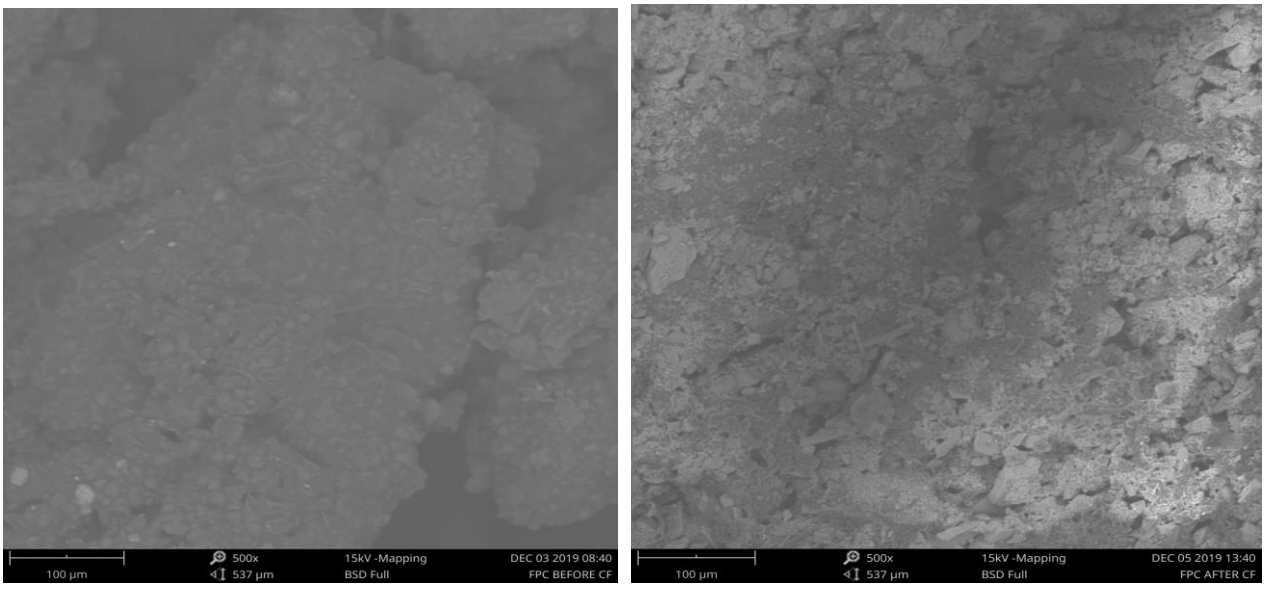

(a) **(b)**

Plate 2: SEM micrograph of TOSA (a) before adsorption (b) after adsorption

3.4 Energy dispersive X-ray (EDX) analysis of BSGA and TOSA

The EDX analysis revealed that the primary elements present in BSGA and TOSA prior to the adsorption procedure were silver, phosphorus, iodine, and carbon (Figures 3ai and bi). However, following adsorption, the primary elements were carbon, silicon, calcium, and aluminium (Figure 3aii and bii). Given that calcium is present in the mashing water, the high atomic concentration of calcium was anticipated (Marcos et al., 2020). The analysis helps estimate biomass's calorific value and assess the environmental impact of the material (Saidur et al., 2011).

Novelty Journals

ISSN 2394-9716

International Journal of Novel Research in Interdisciplinary Studies
Vol. 12, Issue 4, pp: (8-29), Month: July – August 2025, Available at: www.noveltyjournals.com

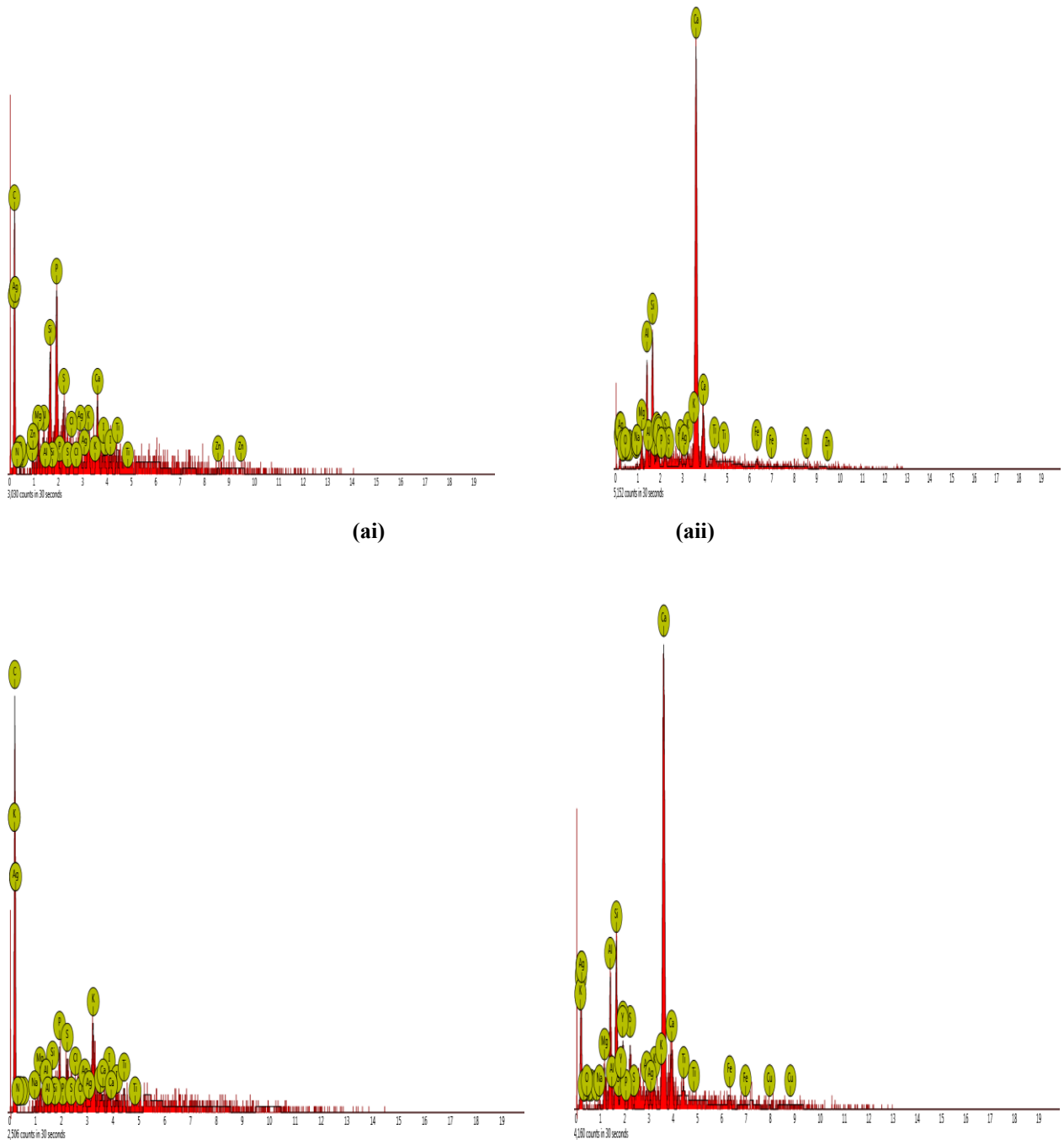

(ai) **(aii)**

(bi) **(bii)**

Figure 3: EDX graph of BSGA (a_i) before adsorption (a_{ii}) after adsorption and TOSA (bi) before adsorption (bii) after adsorption.

3.5 Design Matrix and Experimental Results

The experimental (Exp) and anticipated (Pre) values for the removal efficiency of lead (Pb) and arsenic (As) from paint wastewater are displayed in Table 3 of the response surface methodology design matrix. It included the results of 20 experimental runs in total as well as the RSM-predicted findings for the removal efficiencies of Pb and As using TOSA and BSGA, respectively.

Novelty Journals

ISSN 2394-9716

International Journal of Novel Research in Interdisciplinary Studies
Vol. 12, Issue 4, pp: (8-29), Month: July – August 2025, Available at: www.noveltyjournals.com

Table 3: CCD for Paint wastewater, using BSGA and TOSA

Std	Run	A Conc. (g)	B pH	C Time (Min)	BSGA				TOSA			
					As Removal (%)		Pb Removal (%)		As Removal (%)		Pb Removal (%)	
					Exp.	Pre	Exp	Pre	Exp.	Pre.	Exp.	Pre.
6	1	5	2	50	57.92	57.19	57.61	56.77	75.36	75.68	73.66	73.99
1	2	3	2	30	50.00	50.42	48.05	48.53	67.12	66.80	65.31	65.00
11	3	4	2	40	64.62	63.51	63.42	62.32	84.11	82.06	82.41	80.36
19	4	4	4	40	66.84	68.36	65.64	67.16	87.22	87.84	85.53	86.15
10	5	5	4	40	65.43	64.87	64.23	63.83	84.52	83.39	82.82	56.03
20	6	4	4	40	66.84	63.36	65.64	67.16	87.22	87.84	85.53	86.15
7	7	3	6	50	42.20	42.93	41.02	41.71	58.06	57.72	56.36	81.69
16	8	4	4	40	66.84	68.36	65.64	67.16	87.22	87.84	85.53	86.15
9	9	3	4	40	62.92	58.91	61.72	57.55	76.05	75.31	74.35	73.61
3	10	3	6	30	40.22	42.09	39.01	40.99	56.01	56.16	54.29	54.43
12	11	4	6	40	62.61	59.16	61.41	57.94	75.12	75.31	73.42	73.60
4	12	5	6	30	46.32	46.47	45.12	45.25	61.33	60.55	59.63	58.86
17	13	4	4	40	66.84	68.36	65.64	67.16	87.22	87.84	85.53	86.15
5	14	3	2	50	48.66	49.65	47.46	48.47	62.67	63.92	61.03	62.27
18	15	4	4	40	66.84	68.36	65.64	67.16	87.22	87.84	85.53	86.15
2	16	5	2	30	48.02	48.45	46.80	47.25	67.04	67.85	65.34	66.14
13	17	4	4	30	63.24	60.37	62.04	59.00	80.34	80.49	78.64	78.78
15	18	4	4	40	66.84	68.36	65.64	67.16	87.22	87.84	85.53	86.15
8	19	5	6	50	56.08	56.80	54.88	55.54	72.03	72.82	70.27	71.05
14	20	4	4	50	66.85	65.15	65.65	64.12	87.21	85.19	85.52	83.51

3.6 Final equation in terms of coded factors

The CCD displayed in Table 2 made it possible to create a mathematical equation in which the anticipated outcomes, Y, were evaluated as a function of adsorbent dosage (A), pH (B), and settling time (C). Equations 8 through 11 were used to calculate Y as the sum of three one-order effects (in terms of A, B, and C), three interactive effects (AB, AC, and BC), and three second-order effects (A2, B2, and C2). After eliminating irrelevant variables as shown in Equations 8 and 9 for percentage As and Pb removal using BSGA and Equations 10 and 11 for percentage As and Pb removal using TOSA, a second-order polynomial model was created utilizing the observed data in terms of coded factors using RSM. ANOVA was then used to evaluate the goodness of fit of the acquired results. According to Sadri et al. (2010), the factor's synergistic effect is shown by the positive sign in front of the model terms, whereas its antagonistic effect is indicated by the negative sign.

$$Y_{\%\ As\ removal} = +68.36 + 2.98\,A - 2.18\,B + 2.39\,C + 1.59\,AB + 0.3975\,BC - 6.47\,A^2 - 7.04\,B^2 - 5.61C^2 \quad (8)$$

$$Y_{\%\ Pb\ removal} = +67.16 + 3.14A - 2.19\,B + 2.56\,C + 2.39\,AC - 6.47\,A^2 - 7.03\,B^2 - 5.60\,C^2 \quad (9)$$

$$Y_{\%\ As\ removal} = +87.84 + 4.04\,A - 3.37\,B + 2.35\,C + 0.8350\,AB + 2.68\,AC + 1.11\,BC - 8.49\,A^2 - 9.16\,B^2 - 5.00\,C^2 \quad (10)$$

$$Y_{\%\ Pb\ removal} = +86.15 + 4.04\,A - 3.38\,B + 2.36\,C + 0.8237\,AB + 2.65\,AC + 1.08\,BC - 8.50\,A^2 - 9.17\,B^2 - 5.01\,C^2 \quad (11)$$

3.7 ANOVA for % removal of As and Pb using BSGA and TOSA

The ANOVA findings for the % elimination of As and Pb using BSGA and TOSA are displayed in Table 4. With respect to As and Pb, the model's F-value of 29.12, 28.84 using BSGA and 157.19, 158.92 using TOSA suggests that the model is significant within the parameters of the experiment. An F-value this large could only be the result of noise with a 0.01% chance (Ji et al., 2024). Model terms are significant if the P-value is less than 0.0500 (Moghadam et al., 2010). The model's P-value is less than 0.0001, which suggests that it is significant. According to Boutra et al. (2022), a P-value of more than 0.100 suggests that the model terms are not significant. All of the model terms for As and Pb removal using TOSA are significant model terms, whereas model terms AB and BC were insignificant model terms for As removal using BSGA. Similarly, all of the model terms for Pb removal using BSGA were unimportant. The adjusted R2 of 0.9302, 0.9283, 0.9867, and 0.9868, respectively, for As and Pb removal percentages using BSGA and TOSA, were in close agreement with the predicted R2 of 0.8040, 0.7930, for As and Pb removal % using BSGA, and 0.9436, 0.9448, for As and Pb removal % using TOSA, since the difference between them is less than 0.2 (Gadeka et al., 2019). The model's adequacy is further confirmed by the appropriate precision of 15.0275, 14.7181 for As and Pb using BSGA and 35.901, 35.9988 for As and Pb using TOSA. When the adequate precision is more than four, the model is considered adequate (Moghadam et al., 2010; Muntean et al., 2023).

The coefficient of variance (C. V) 4.20, 4.36, 1.67, and 1.70% for the removal efficiency of As and Pb, using BSGA and TOSA, respectively were less than 10 %. This still affirmed the model's accuracy. The low values of the standard deviations (2.47, 2.51, 1.28, and 1.27), respectively also verified the authenticity of the model.

Table 4: ANOVA for percentage removal of As and Pb using BSGA and TOSA

Source	BSGA				TOSPA			
	F-value		P-vale		F-value		P-value	
	As	Pb	As	Pb	As	Pb	As	Pb
Model	29.12	28.34	<0.0001	<0.0001	157.19	158.92	<0.0001	<0.0001
A-Dosage	14.50	15.58	0.0034	0.0027	99.94	100.94	<0.0001	<0.0001
B-pH	7.77	7.59	0.0192	0.0203	69.85	70.64	<0.0001	<0.0001
C-Time	9.35	10.37	0.0121	0.0092	33.84	34.57	0.0002	0.0002
AB	3.30	2.42	0.0994	0.1506	3.42	3.36	0.0941	0.0967
AC	7.40	7.25	0.0216	0.0226	35.17	34.68	0.0001	0.0002
BC	0.2068	0.0475	0.6590	0.8318	6.04	5.82	0.0338	0.0366
A^2	18.86	18.20	0.0015	0.0016	121.62	123.08	<0.0001	<0.0001
B^2	22.27	21.49	0.0008	0.0009	141.57	143.24	<0.0001	<0.0001
C^2	14.14	13.64	0.0037	0.0042	42.20	42.69	<0.0001	<0.0001
	As		Pb		As		Pb	
Lack of fit	61.12		63.22		16.31		16.15	
Std. Deviation	2.47		2.51		1.28		1.27	
R^2	0.9632		0.9623		0.9930		0.9931	
Adj. R^2	0.9302		0.9283		0.9867		0.9868	
Pred. R^2	0.8040		0.7939		0.9436		0.9448	
C.V. %	4.20		4.36		1.67		1.70	
Adeq. Prec.	15.0275		14.7181		35.0901		35.9988	

3.8 Diagnostic Plots for As and Pb Removal Efficiency using BSGA and TOSA

Using BSGA and TOSA, respectively, the data was examined to look for correlations between the experimental (Yexperiment) and projected responses, as shown in Figures 4 a, b, c, and d for the percentage removal of As and Pb. When compared to the experimental data, a model must be able to predict the reaction with a reasonable degree of accuracy to be considered reliable (Anyaene et al., 2022). As can be shown, for the two adsorbents (BSGA and TOSA) tested, the data points were distributed nearly in a straight line. This indicates that there is a good correlation between the experimental and expected values of the response, and the analysis's underlying presumptions were valid (Muntean et al., 2023). This outcome also suggests that the quadratic model that was chosen to assume the response variables for the experimental data was suitable.

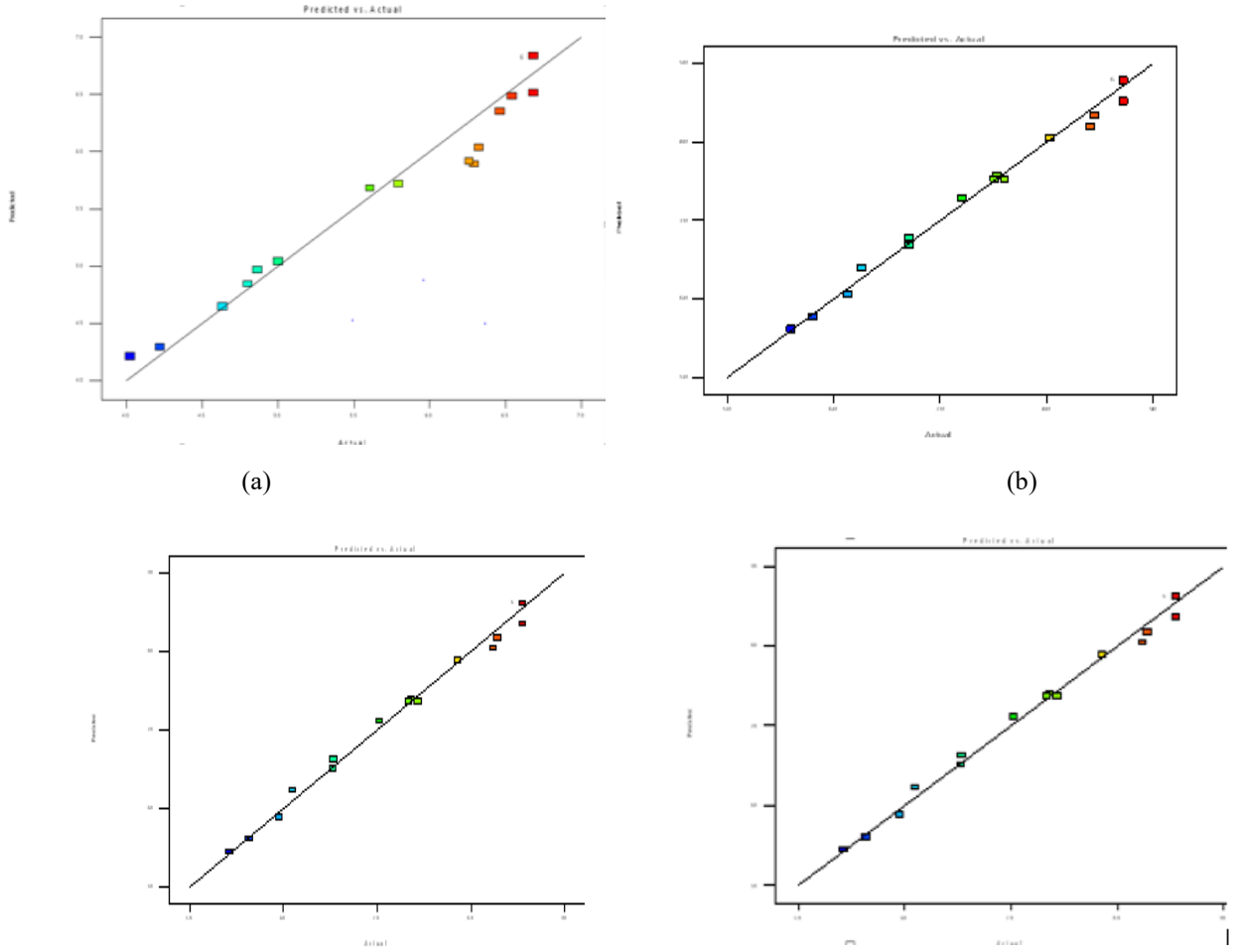

(a) (b)

(c) (d)

Figure 4: Predicted vs Actual (a) % As removal using BSGA (b) % As removal using TOSPA (c) % Pb removal using BSGA (d) % Pb removal using TOSA.

3.9 Three-Dimensional Response Surface Plots

A three-dimensional response surface graph was created using RSM to show the connections between the experimental factors and the related responses (Figure 5a1 to 5d3). In this method, the response surface's curvature represents the importance of the interactions between the experimental variables. Here, two factors were varied over the experimental range while one variable remained constant in order to examine the influence of the experimental factors. The curve illustrates the nonlinear relationship between response (As and Pb removal efficiency) and variables (adsorbent dosage, pH, and settling time).

Novelty Journals

ISSN 2394-9716

International Journal of Novel Research in Interdisciplinary Studies
Vol. 12, Issue 4, pp: (8-29), Month: July – August 2025, Available at: www.noveltyjournals.com

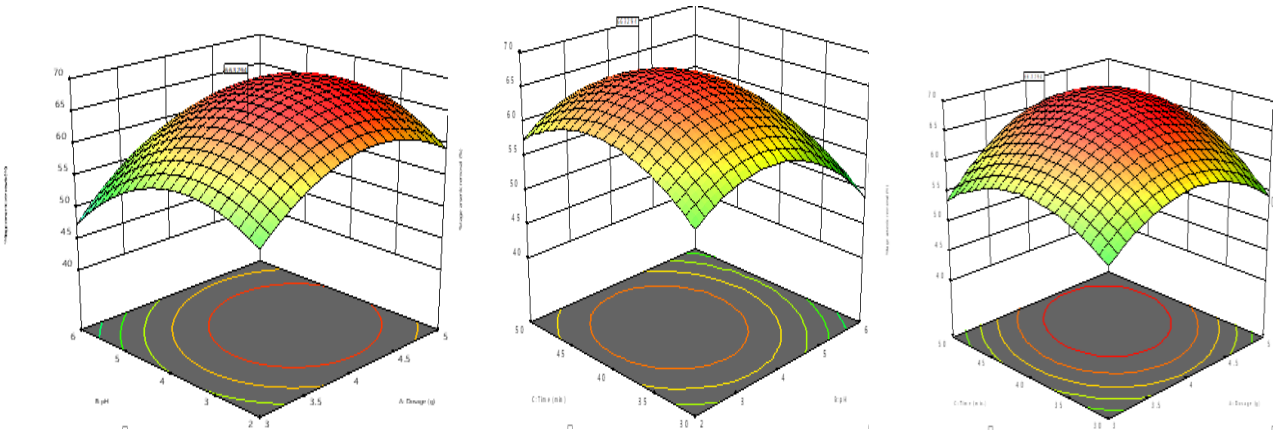

(a1) (a2) (a3)

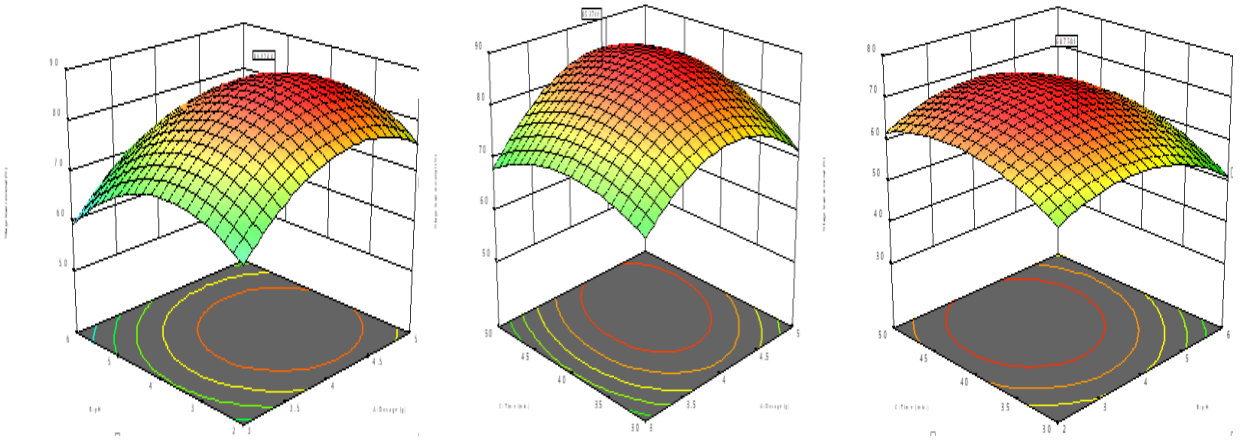

(b1) (b2) (b3)

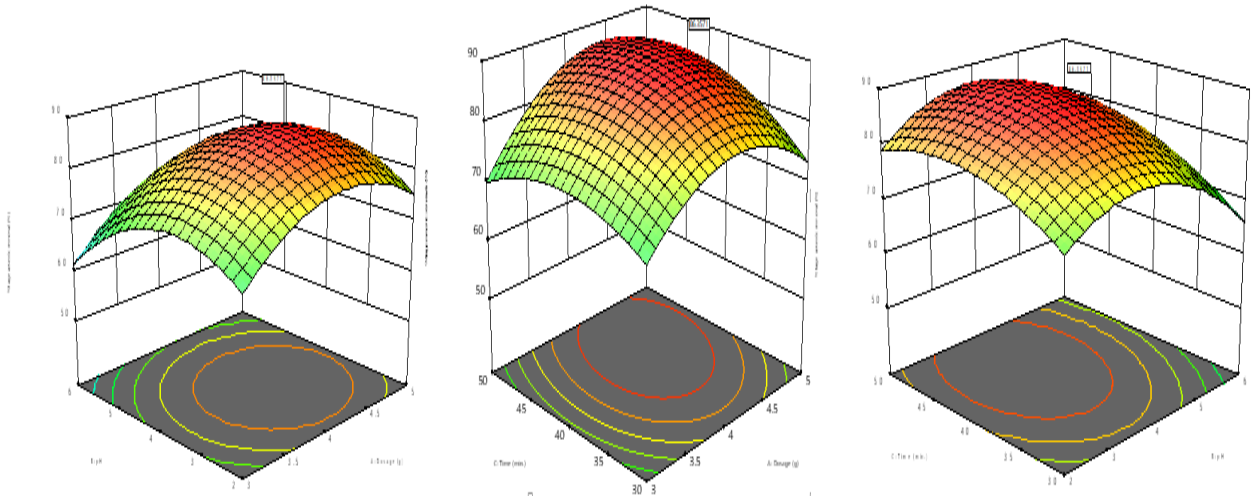

(c1) (c2) (c3)

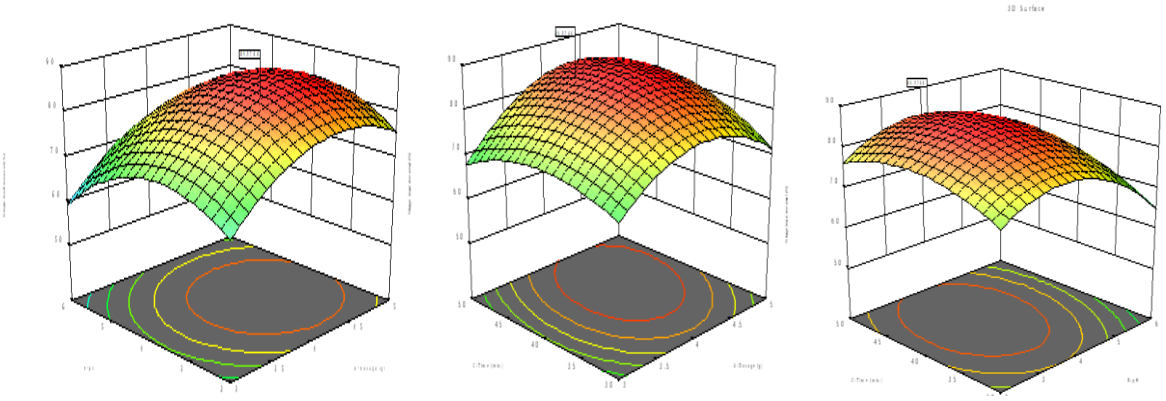

(d1) (d2) (d3)

Figure 5: Three-dimensional surface plot for (a) % As removal versus (a1) pH and dosage (a2) Time and dosage (a3) Time and pH using BSGA (b) % Pb removal versus (b1) pH and dosage (b2) Time and dosage (b3) Time and pH using BSGA (c) % Pb removal versus (c1) pH and dosage (c2) Time and dosage (c3) Time and pH using TOSA (d) % Pb removal versus (d1) pH and dosage (d2) Time and dosage (d3) Time and pH using TOSA.

3.10 Optimum Parameters and Removal Efficiencies of Contaminants

Design Expert version 12.0 was used for optimization to maximize the process variables for the pollutants' removal efficiencies and, as a result, acquire the ideal values for removal efficiencies. Process optimization looks for a factor-level combination that simultaneously satisfies the requirements set for each response (Khelifi et al., 2022). The use of numerical optimization was made. The intended maximum goal was established for every element and response in numerical optimization. To efficiently maximize the function, these objectives were integrated into an overall desirability function. Table 5 displays the ideal adsorbent dosage, pH, and settling time values together with the related pollutant removal efficiencies as predicted by the model. Because BSGA has a stronger affinity for Pb than As employing BSGA in paint effluent resulted in a high value for Pb removal efficiency. Additionally, the application of TOSA produced high levels of Pb and As elimination percentages. When BSGA was utilized as an adsorbent, the removal efficiencies of As were comparatively poor.

Table 5: Optimum Parameters of As and Pb for the Paint Waste Water

Samples	Optimum dosage (g/l)	Optimum pH	Optimum Time (Min.)	Optimum As (%)	Optimum Pb (%)
BSGA	4.12	2.60	40.35	66.33	83.37
TOSA	4.00	4.00	40.00	86.36	85.37

3.11 Langmuir, Freundlich, and Temkin isotherm study for heavy metal removal from paint wastewater

The Langmuir, Freundlich, and Temkin isotherm model of As and Pb removal from the Paint wastewater sample is displayed in Figures 6a through c. Table 6 shows the adsorption parameters of the model. The Langmuir isotherm for the removal of As and Pb from paint effluent has an R2 value of determination of 0.995 and 0.993, respectively. In contrast to the results derived using the Freundlich and Temkin isotherm models, these values were high. According to Albana et al. (2018), the adsorption intensity, n, which represents the energy of the heterogeneity of the adsorbate site and the relative distribution of the active sites for As and Pb, was less than 1, indicating poor adsorption properties. The adsorption capacity in the Freundlich isotherm of zero, denoted by the constant KF, indicates that the model did not adequately fit the equilibrium data (Tatsumi et al., 2021). As and Pb's Langmuir isotherms' separation factors (RL) fell between 0 and 1, indicating a satisfactory fit with the equilibrium data. The data show conclusive evidence that As and Pb adsorption follows the Langmuir isotherm. The possibility of heavy metal sorption onto polymers through chemisorption is revealed by the fit of the observed data to the Langmuir model (Ali & Maryam, 2020).

Novelty Journals

ISSN 2394-9716

International Journal of Novel Research in Interdisciplinary Studies
Vol. 12, Issue 4, pp: (8-29), Month: July – August 2025, Available at: www.noveltyjournals.com

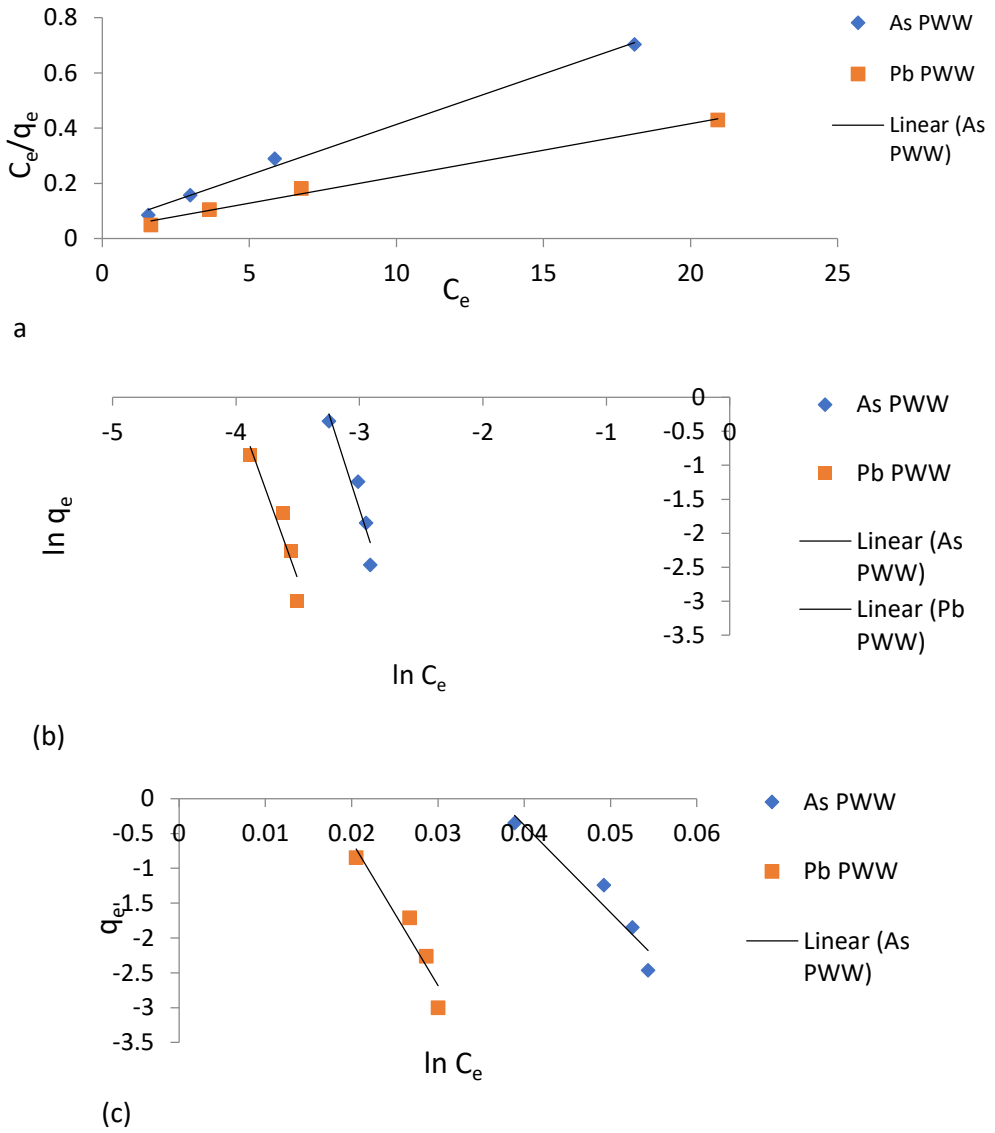

Figure 6: Linear isotherm results (a) Langmuir (b) Freundlich isotherm (c) Temkin isotherm

Table 6: Langmuir, Freundlich, and Temkin isotherm parameters on adsorption mechanism studies for heavy metals removal

Isotherms	**PWW**	
Langmuir	**As**	**Pb**
q_{max} (mg L/mg)	27.322	52.083
K_L (L/mg)	0.772	0.585
R_L^2	0.995	0.993
R_L	0.364	0.577
Freundlich		
K_f (mg/g(L/mg)$^{1/n}$)	0.0000	0.0000
n	-0.1766	-0.1986
R_F^2	0.9001	0.8840
Temkin		
A (L/mg)	-0.008	-0.005
B	4.623	3.523
R^2	0.910	0.910

Novelty Journals

ISSN 2394-9716

International Journal of Novel Research in Interdisciplinary Studies
Vol. 12, Issue 4, pp: (8-29), Month: July – August 2025, Available at: www.noveltyjournals.com

3.12. Kinetics studies for As and Pb removal from PWW

Designing effective adsorption studies hinges on understanding the adsorption's kinetics, which calls for the employment of appropriate kinetics models (Jianlong & Xuaan, 2020). The experimental data were fitted using linear regression of pseudo-first order, pseudo-second order, Elovich kinetics models, and intra-particle diffusion model; the plots for As and Pb are displayed in Figures 7 a-h. Table 7 displays the kinetics models' parameters. It was discovered that the pseudo-first order kinetic equation did not match the experimental results due to poor R2 values for the two polymers utilized, TOSA and BSGA. In comparison to the Elovich model, very high values of R2 (>0.97) were achieved for the pseudo-second-order kinetic model BSGA and TOSA for the removal of As and Pb. This validates the pseudo-second-order kinetics model for heavy metals, which is based on the chemisorption theory (Ali & Maryam, 2020). As has a great affinity for the adsorbents, as indicated by the high KF2 values for the two adsorbents (Javid et al., 2022). Figures 7g and h displayed the intra-particle plots for As and Pb removal for the BSGA and TOSA under study. The low value of KF3 suggests that the adsorbents were less affected by the boundary layer when it came to the adsorption of As. The plotted spots' minimal departure from the origin indicates that the adsorption mechanism is mostly an intra-particle mechanism. The model's correlation coefficients were strong (>0.9), indicating that it does a good job of explaining the experimental data.

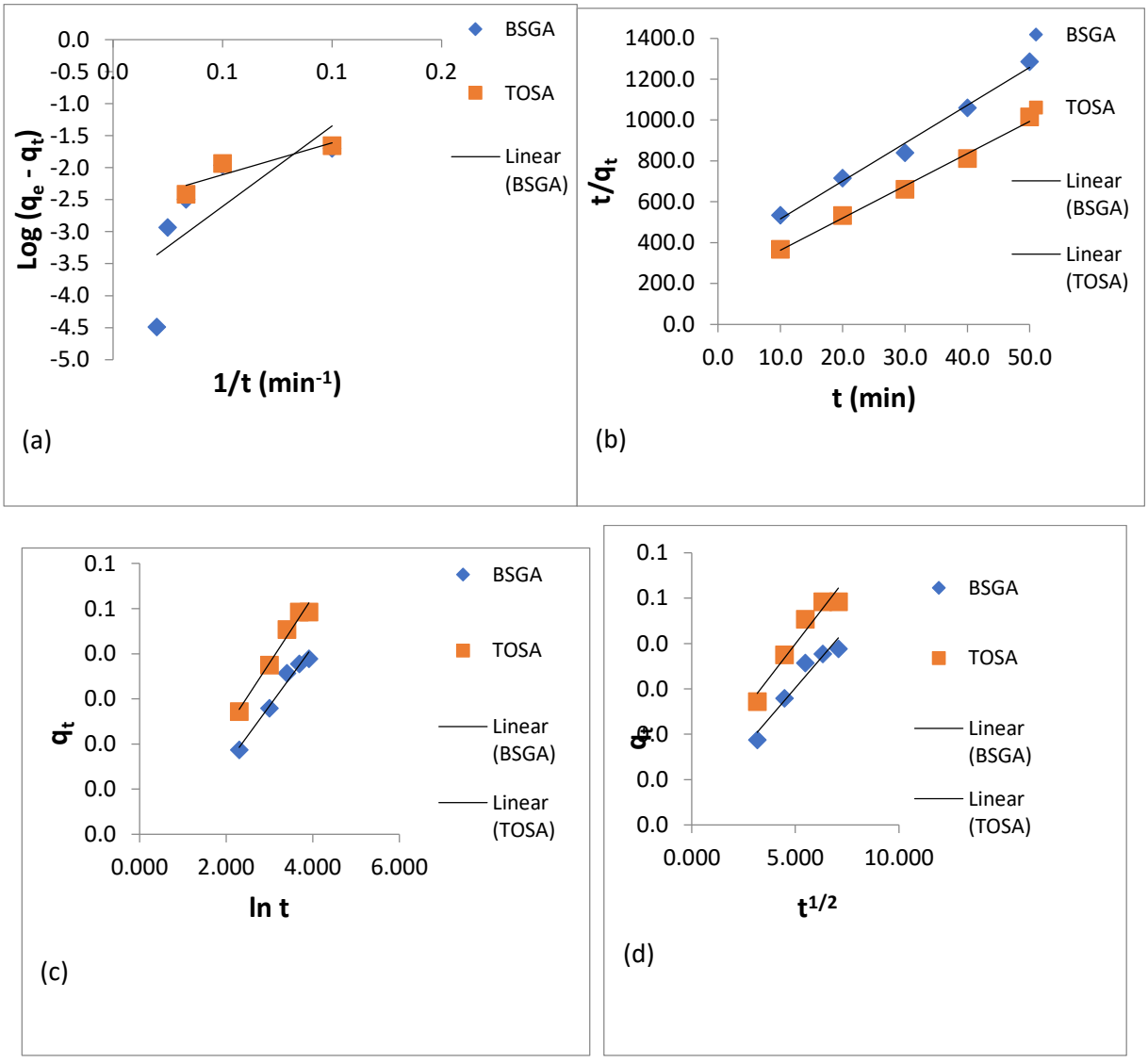

Novelty Journals

ISSN 2394-9716

International Journal of Novel Research in Interdisciplinary Studies
Vol. 12, Issue 4, pp: (8-29), Month: July – August 2025, Available at: www.noveltyjournals.com

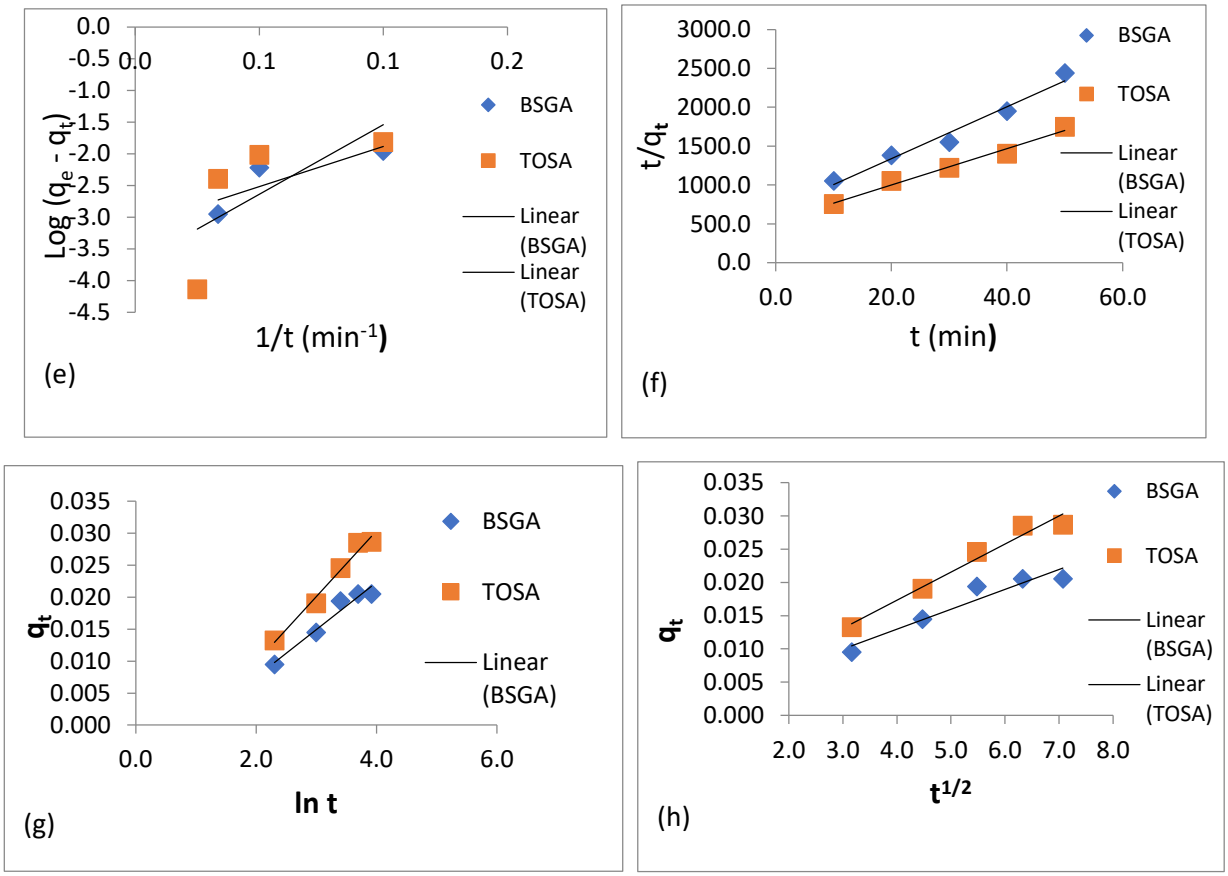

Figure 7: Linear regression plots for kinetic models at pH of 4 (a) PFO for As removal (b) PFO for Pb removal (c) PSO for As removal (d) PSO for Pb removal (e) Elovich kinetic model for As removal (f) Elovich kinetic model for Pb removal (g) Intra-particle diffusion model fo As removal (h) Intra-particle diffusion model for Pb removal.

Table 7: Kinetic Models Parameters for As and Pb.

Pseudo-first-order kinetic for As					
Adsorbent	q_e, exp (mg/g)	q_e, cal (mg/g)	K_{F1} (min^{-1})	R^2	RMS (%)
BSGA	0.0389	0.00014	57.973	0.5502	49.824
TOSA	0.0492	0.00244	23.060	0.82	47.520
Pseudo-first-order kinetics for Pb					
Adsorbent	q_e, exp (mg/g)	q_e, cal (mg/g)	K_{F1} (min^{-1})	R^2	RMS (%)
BSGA	0.0205	0.0007	29.2159	0.7282	48.2854
TOSA	0.0286	0.0002	50.5439	0.4843	49.6783

Pseudo-second-order kinetics for As						
Adsorbent	q_e, exp (mg/g)	q_e, cal (mg/g)	K_{F2} (g/mg min)	R^2	h (mg/g min)	RMS (%)
BSGA	0.0205	0.0299	22436.4063	0.9718	20.1255	23.0487
TOSA	0.0286	0.0428	12472.9686	0.9835	22.8808	24.8780

Pseudo-second-order kinetics for Pb						
Adsorbent	q_e, exp (mg/g)	q_e, cal (mg/g)	K_{F2} (g/mg min)	R^2	h (mg/g min)	RMS (%)
BSGA	0.0389	0.0540	6142.6584	0.9865	17.9343	19.4519
TOSA	0.0492	0.0635	3238.5762	0.9940	13.0588	14.5326

Elovich Kinetics for As			
Adsorbent	a	b	R^2
BSGA	3.03E-02	76.336	0.9759
TOSA	2.20E-02	68.493	0.976

Elovich kinetics for Pb			
Adsorbent	a	b	R^2
BSGA	1.98E-02	135.135	0.9564
TOSA	2.94E-02	97.087	0.9785
Intra-particle diffusion model for As			
Adsorbent	C	K_{F3} (mgg^{-1} $min^{1/2}$)	R^2
BSGA	0.0036	0.0053	0.9382
TOSA	0.0103	0.0059	0.9391
Intra-particle diffusion model for Pb			
Adsorbent	C	K_{F3} (mgg^{-1} $min^{1/2}$)	R^2
BSGA	0.001	0.003	0.9142
TOSA	0.0004	0.0042	0.9656

4. CONCLUSIONS

This study used extracts from Telfairia occidentalis seed powder and biosorbents made from brewer's waste grain to examine the adsorption of AS and Pb. The outcomes demonstrated that both biosorbents had notable lead and arsenic adsorption capabilities. While TOSA showed good adsorption capacities for both pollutants, BSGA showed better adsorption capabilities for lead than for arsenic. This study demonstrates how these biosorbents can be used to remove lead and arsenic from tainted paint effluent in an economical and environmentally responsible manner. To safeguard and maintain our ecosystem, industrial effluents must be cleansed of harmful pollutants before being released into our terrestrial or aquatic environments.

List of abbreviations

TOSA - *Telfairia occidentalis* adsorbent

BSGA - Brewers' spent grain adsorbent

Pb – Lead

As – Arsenic

RSM – Response surface methodology

K_1 – Rate constant of first-order adsorption model

K_2 – Rate constant of first-order adsorption model

k_{int} - Intra-particle diffusion rate constant

CCD – Central composite design

WHO – World Health Organization

EPA – Environmental Protection Authority

PWW – Paint wastewater

AAS - Atomic Absorption Spectrometer

FTIR - Fourier transformed infra-red spectrophotometer

EDX - Energy dispersive X-ray

SEM - Scanning electron microscopy

OFAT - One-factor-at-a-time

TOSP - *Telfairia occidentalis* seed powder

BSGP - Brewers' spent grain powder

Declarations

Data availability statement

The datasets generated during and/or analyzed during the current study are available from the corresponding author upon reasonable request.

Ethics declarations

The collection of plants used in this study complies with local or national guidelines with no need for futher affirmation.

Competing interest

The authors declare that they have no known competing financial interests or personal relationships that could have appeared to influence the work reported in this paper.

Funding

The authors received no funding for this study.

Authors contributions

H.I.A, D.O.O – Drafting of the article, Data sharing, technical support, Funding acquisition, experimental work, analysis, interpretation of data, and materials support

H.I.A. N.J.E- Conceptualization, methodology, acquisition of data, funding acquisition, experimental work, supervision, drafting of the article, and final approval.

Acknowledgement

The authors wish to thank the management and technical staff of the Departments of Chemical Engineering Caritas University Enugu Nigeria for granting the authors access to their laboratories and workshops.

REFERENCES

[1] Abugu, H. O., Alum, O. L., Ihedioha, J. N., Ezugwu, A. L., Ucheana, I. A., Ali, I. J., & Eze, S. I. (2023). Sequestration of Pb2+ from aqueous solution using bio-based-alkaline modified sorbent from waste Irvingia gabonensis seed husk. *Water Practice & Technology*, *18*(11), 2495-2513.

[2] Adegoke, H. I., Ashola, M. O., & Audu, M. F. (2023). Kinetics and equilibrium adsorption studies of chromium (VI) and iron (III) from aqueous solution systems using hydroxyapatite, activated carbon, and their composites, *Ife Journal of Science*, *25*(1), 095-113.

[3] Ahmad, M., Ahmed, S., & Ikram, S. (2015). Adsorption of Heavy Metal Ions: Role of Chitosan and Cellulose for Water Treatment. *International Journal of Pharmacognosy*, *2*(6), 280–289. https://doi.org/10.13040/IJPSR.0975-8232.I JP.2(6).280-289

[4] Ainul& Nazirah, (2020). Paint Waste Management Industry. *Journal of Advanced Research in Business and Management Studies* 20, (1), 28-33.

[5] Alalwan, H. A., Kadhom, M. A., & Alminshid, A. H. (2020). Removal of heavy metals from wastewater using agricultural byproducts. *Journal of Water Supply: Research and Technology—AQUA*, *69*(2), 99-112.

[6] Anyaene, H. I., Onukwuli, O. D., Obiora-okafo I. A., Babayemi, A. K., (2022).Response Surface Methodology Approach to Optimization of Process Parameters for Coagulation-Flocculation of Paint Wastewater using *Telfairia occidentalis seed*. *World Journal of Innovative Research,* 12 (2), 42-50.

[7] Ayawei, N., Ebelegi, A. N., & Wankasi, D. (2017). Modelling and Interpretation of Adsorption Isotherms. In *Journal of Chemistry* 2017, 3039817. Hindawi Limited. https://doi.org/10.1155/2017/3039817

[8] Batool F. S., Masood, N., Farooqi, A. (2024). Techniques of Arsenic remediation on household and Commercial Scale In Kumar, N., Hashmi, M. Z., Wang S. (eds) Arsenic Toxicity Remediation. Emerging Contaminants and Associated Treatment Technologies. Springer, Cham. https//doi.org/10.1007/978-3-031-52614-5_14.

[9] Bayero, A. S., Datti, Y., Lado, U. A., Yahya, A. T., Musbahu, L., Rabiu, N. N., Nura, T., Adamu, G. A., Umar, A., and Ahmed, U. U. (2020). Efficiency of Fluted Pumpkin Plant (*Telfairia Occidentalis*) in the Phytoremediation of Wastewater Effluent from Sharada Industrial Area, Kano State, Nigeria. *FUDMA Journal of Sciences (FJS),* 4 (1), 594 – 599.

[10] Bilal, M., Ihsanullah, I., Younas, M., & Shah, M. U. H. (2021). Recent advances in applications of low-cost adsorbents for the removal of heavy metals from water: A critical review. *Separation and Purification Technology*, *278*, 119510.

[11] Boutra, B., Sebti, A., & Trari, M. (2022). Response surface methodology and artificial neural network for optimization and modeling the photodegradation of organic pollutants in water. *International Journal of Environmental Science and Technology*, *19*(11), 11263-11278.

[12] Chakraborty, R., Asthana, A., Singh, A. K., Jain, B., & Susan, A. B. H. (2022). Adsorption of heavy metal ions by various low-cost adsorbents: a review. *International Journal of Environmental Analytical Chemistry*, *102*(2), 342-379.

[13] Chime, T. O., Onyema, C. C., & Ejikeme, P. C. N. (2016). Removal of lead from paint effluent using low-cost activated adsorbent (fluted pumpkin seed shells). *IJERT Int. J. Eng. Res. Technol*, *5*(9), 676-683.

[14] Chukwuma, O. U., Uchenna, O. M., Ogonna, U. S., & Chinedu, O. S. (2022). The Effects of Effluents'Discharge from Some Paint Industries on Soil's Physicochemical Properties and Bio-attenuation of Polluted Soil. *Industrial and Domestic Waste Management*, *2*(2), 46-60.

[15] Dagne Bekele Bahiru, (2020) Determination of Heavy Metals in Wastewater and Their Toxicological Implications around Eastern Industrial Zone, Central Ethiopia. Journal of Environmental Chemistry and Ecotoxicology 12(2), 72-79, DOI:10.5897/JECE2019.0453.

[16] Elbana, T. A., Selim, H. M., Akrami, N., Newman, A., Shaheen, S. M., & Rinklebe, J. (2018). Freundlich sorption parameters for cadmium, copper, nickel, lead, and zinc for different soils: Influence of kinetics. *Geoderma*, *324*, 80-88.

[17] Etale, A., Onyianta, A. J., Turner, S. R., & Eichhorn, S. J. (2023). Cellulose: a review of water interactions, applications in composites, and water treatment. *Chemical Reviews*, *123*(5), 2016-2048.

[18] Fahim, I. S., & Said, L. (Eds.). (2023). *Wastewater Treatment: Recycling, Management, and Valorization of Industrial Solid Wastes*. CRC Press.

[19] Gadekar, M. R., & Ahammed, M. M. (2019). Modelling dye removal by adsorption onto water treatment residuals using combined response surface methodology-artificial neural network approach. *Journal of environmental management*, *231*, 241-248.

[20] Gupta, N., Singh, M., Gupta, P., Mishra, P., & Gupta, V. (2023). Heavy Metal Bioremediation and Toxicity Removal from Industrial Wastewater. *Next-Generation Algae: Volume I: Applications in Agriculture, Food and Environment*, 163-193.

[21] Javid, A., Roudbari, A., Yousefi, N., Fard, M. A., Barkdoll, B., Talebi, S. S., ... & Ghadiri, S. K. (2020). Modeling of chromium (VI) removal from aqueous solution using modified green-Graphene: RSM-CCD approach, optimization, isotherm, and kinetic studies. *Journal of Environmental Health Science and Engineering*, *18*, 515-529.

[22] Ji, X., Li, Z., Wang, M., Yuan, Z., & Jin, L. (2024). Response Surface Methodology Approach to Optimize Parameters for Coagulation Process Using Polyaluminum Chloride (PAC). *Water*, *16*(11), 1470.

[23] Jianlong Wang, Xuan Guo, 2020. Adsorption kinetic models: Physical meanings, applications, and solving methods, Journal of Hazardous Materials, 390, 122156.

[24] Joshi, N. C., & Gururani, P. (2022). Advances of graphene oxide-based nanocomposite materials in the treatment of wastewater containing heavy metal ions and dyes. *Current Research in Green and Sustainable Chemistry*, *5*, 100306.

[25] Khelifi, O., Affoune, A. M., Nacef, M., Chelaghmia, M. L., & Laksaci, H. (2022). Response surface modeling and optimization of Ni (II) and Cu (II) ions competitive adsorption capacity by sewage sludge activated carbon. *Arabian Journal for Science and Engineering*, *47*(5), 5797-5809.

[26] Kulkarni, S. J. (2016). Wastewater Treatment for Lead Removal: A Review. *International Journal of Scientific Research in Science, Engineering and Technology*, *1*(1), 272-275.

[27] Lynch, K. M., Steffen, E. J., and Arendt, E. K. (2016). Brewers' spent grain: a review with an emphasis on food and health. *J. Inst. Brew.*, 122: 553– 568. doi: 10.1002/jib.363.

[28] M.A. Aboulhassan, S. Souabi, A. Yaacoubi, and M. Baudu (2014). Treatment of Paint Manufacturing Wastewater by the Combination of Chemical and Biological, *International Journal of Science, Environment and Technology*, 3, (5), 1747 – 1758

[29] Maftouh, A., El Fatni, O., El Hajjaji, S., Jawish, M. W., & Sillanpää, M. (2023). Comparative review of different adsorption techniques used in heavy metals removal in water. *Biointerface Res. Appl. Chem*, *13*, 397.

[30] Mathur, V., & Sherry, P. A (2023). Review on Impact of Heavy Metal on Water Quality and on Aquatic Environment. *International Journal of Innovative Research in Science, Engineering and Technology (IJIRSET),* 12 (1) DOI:10.15 680/IJIRSET.2023.1201016.

[31] Moghaddam, S. S., Moghaddam, M. A., & Arami, M. (2010). Coagulation/flocculation process for dye removal using sludge from water treatment plant: optimization through response surface methodology. *Journal of hazardous materials*, *175*(1-3), 651-657.

[32] Muntean, S. G., Halip, L., Nistor, M. A., & Păcurariu, C. (2023). Removal of metal ions via adsorptionusing carbon magnetic nanocomposites: optimization through response surface methodology, kinetic and thermodynamic studies. *Magnetochemistry*, *9*(7), 163.

[33] Muntean, S. G., Halip, L., Nistor, M. A., & Păcurariu, C. (2023). Removal of metal ions via adsorption using carbon magnetic nanocomposites: optimization through response surface methodology, kinetic and thermodynamic studies. *Magnetochemistry*, *9*(7), 163.

[34] Mwaniki, J. M., Onyatta, J. O., & Yusuf, A. O. (2019). Adsorption of heavy metal ions from aqueous solutions and wastewater using water hyacinth powder. *Adsorption*, *4*(1).

[35] Najamuddin, S. S., Shukri, N. M., Salleh, N. M., Abdullah, W. W., Shohaimi, N. M., Ab Halim, A. Z., & Abdullah, N. H. (2022). Simultaneous Removal of Lead, Cadmium, and Arsenic Ions from Bivalve Species Using Adsorption Method. In *IOP Conference Series: Earth and Environmental Science* (Vol. 1102, No. 1, p. 012013). IOP Publishing.

[36] Nyong, B. E., Ita, O. O., Ita, P. O., & Jones, B. B. (2021). Physico-chemical composition of Telfairia Occidentalis (fluted pumpkin fruit) pulp. *Journal of Research in Pharmaceutical Science*, *7*(6), 14-19.

[37] Obiora-Okafo, I. A., & Onukwuli, O. D. (2017). Optimization of coagulation-flocculation process for colour removal from azo dye using natural polymers: Response surface methodological approach. *Nigerian Journal of Technology*, *36*(2), 482-495.

[38] Olumakinde, A., Otitoloju, K., & Ezemba, C. C. (2019). Growth of Abelmoshus esculentus L.(Okra) and Telfairia occidentalis Hook F.(Fluted Pumpkin) Treated with Beauty Salon Wastewater. *American Journal of BioScience*.

[39] Podgorski, J. & Berg M., 2020. The global threat of arsenic in groundwater. Science, 368 (649), 845- 850.

[40] Rana, A., Haseeb, Z., Baig, A., Naseer, N., & Bilal, S. (2022). Monitoring of Environment and Human Health Impact Assessment of Paint Industry. *SSRG Int. J. Agric. Environ. Sci*, *9*, 54-61.

[41] Rehman A, Ullah H, Khan RU, Ahmad I (2013). Population-based study of heavy metals in medicinal plant Capparis decidua. International Journal of Pharmacy and Pharmaceutical Sciences, 5(1):108-113.

[42] S. A., & KANGALE, K. A (2020) Review on Removal of Heavy Metals by Using Low-Cost Adsorbents with Reference to Electroplating Industry. *International Journal of Innovations in Engineering Research and Technology*, *6*(4), 1-7.

[43] Saini, S., Gill, J. K., Kaur, J., Saikia, H. R., Singh, N., Kaur, I., & Katnoria, J. K. (2020). Biosorption is as environmentally friendly technique for heavy metal removal from wastewater. *Fresh water pollution dynamics and remediation*, 167-181.

[44] Sall, M.L., Diaw, A.K.D., Gningue-Sall, D., Aaron, S.E., Aaron, J.J., (2020). Toxic heavy metals: Impact on the environment and human health, and treatment with conducting organic polymers, a review. *Environ. Sci. Pollut. Res*., 27, 29927–29942.

[45] Samuel A. E., Nwankwo I. C., Ezebor F. and Ojuolape A. A. (2019), Adsorption of chromium by brewers spent grain -gpoly (acrylic acid-co-acryl amide) from electroplating effluent. *African Journal of Pure and Applied Chemistry,* Vol. 13(5), 64-71. DOI: 10.5897/AJPAC2017.0734

[46] Sana, I., Lian Y. H., Huijuan, Z., Jing, W., Meng, Y. (2017). Composition and Nutrient Value Proposition of Brewer's Spent Grain. *Journal of Food Science*, 82 (10), 2232-2242. https//doi.org/10.1111/1750-3841.13794.

[47] Schmidt, A. R., Dresch, A. P., Alves Junior, S. L., Bender, J. P., & Treichel, H. (2023). Applications of Brewer's Spent Grain Hemicelluloses in Biorefineries: Extraction and Value-Added Product Obtention. *Catalysts*, *13*(4), 755. MDPI AG. Retrieved from http://dx.doi.org/10.3390/catal13040755

[48] Shah, G. M., Nasir, M., Imran, M., Bakhat, H. F., Rabbani, F., Sajjad, M., ... & Song, L. (2018). Biosorption potential of natural, pyrolyzed, and acid-assisted pyrolyzed sugarcane bagasse for the removal of lead from contaminated water. *PeerJ*, *6*, e5672.

[49] Shrestha, R., Ban, S., Devkota, S., Sharma, S., Joshi, R., Tiwari, A. P., ... & Joshi, M. K. (2021). Technological trends in heavy metals removal from industrial wastewater: A review. *Journal of Environmental Chemical Engineering*, *9*(4), 105688.

[50] Tatsumi, T., Tahara, Y., & Matsumoto, M. (2021). Adsorption of metallic ions on amidoxime-chitosan/cellulose hydrogels. *Separations*, *8*(11), 202.

[51] Ullah, R., Ullah, T., & Khan, N. (2023). Removal of Heavy Metals from Industrial Effluents using Burnt Potato Peels as Adsorbent. *J. Appl. Organomet. Chem.*, *3*(4), 284-293.

[52] Ungureanu, E. L., Mocanu, A. L., Stroe, C. A., Panciu, C. M., Berca, L., Sionel, R. M., & Mustatea, G. (2023). Agricultural byproducts used as low-cost adsorbents for removal of potentially toxic elements from wastewater: a comprehensive review. *Sustainability*, *15*(7), 5999.

[53] Vandana M., & Poonam S. (2023). A Review on Impact of Heavy Metal on Water Quality and Aquatic Environment. International Journal of Innovative Research in Science, Engineering and Technology (IJIRSET), 12 (1) DOI:10. 15680/IJIRSET.2023.1201016

[54] Vishali, S., & Kavitha, E. (2021). Application of membrane-based hybrid process on paint industry wastewater treatment. In *Membrane-based hybrid processes for wastewater treatment* (pp. 97-117). Elsevier.

[55] Vo, T. S., Hossain, M. M., Jeong, H. M., & Kim, K. (2020). Heavy metal removal applications using adsorptive membranes. *Nano convergence*, *7*(1), 36.

[56] Wirnkor, V. A., Ngozi, V. E., Jr, M. H., & Ndubuisi, I. G (2020). Effect of Adsorption Parameters of Organics from Vegetable Oil Industry Effluents onto Adsorbents from Telfairia Occidentalis Waste. *Science View Journal*, 1 (2), 93-99.

[57] Yi Su, Marco Wenzel, Silvia Paasch, Markus Seifert, Wendelin Böhm, Thomas Doert, and Jan J. Weigand (2021). Recycling of Brewer's Spent Grain as a Biosorbent by Nitro-Oxidation for Uranyl Ion Removal from Wastewater *ACS Omega 6* (30), 19364-19377 DOI: 10.1021/acsomega.1c00589